LTH 1021

Low momentum propagators at two loops in gluon mass model

J.A. Gracey,
Theoretical Physics Division,
Department of Mathematical Sciences,
University of Liverpool,
P.O. Box 147,
Liverpool,
L69 3BX,
United Kingdom.

August, 2014.

Abstract. We compute the two loop corrections to the gluon propagator for low momentum in a gluon mass model. This model has recently been proposed as an alternative to the Gribov construction in the way it handles Gribov copies in the gauge fixing. The corrections provide improvements for estimating the point where the gluon propagator freezes in relation to lattice data.

1 Introduction.

The low momentum properties of the propagators of gluons and Faddeev-Popov ghosts in Quantum Chromodynamics (QCD) has been the subject of intense interest in recent years. See, for example, [1, 2, 3, 4, 5, 6, 7, 8, 9, 10, 11]. The main motivation for such studies rests in their relation to colour confinement. In a non-abelian gauge theory gluons have a fundamental style of propagator at high energy indicating an effective particle interpretation. Specifically the fields are effectively massless and asymptotically free. That such vector gauge bosons are not observed in nature is indicative of a deeper structure from the point of view of the full propagator. In other words taken over the whole energy spectrum the gluon propagator does not have a fundamental structure with a simple pole at zero or a non-zero value. Instead recent lattice gauge theory studies have reached the consensual picture that the propagator not only does not have a pole but it freezes at zero momentum to a non-zero value [1, 2, 3, 4, 5, 6, 7, 8, 9]. This positivity violating form is consonant with a confined gluon and hence no free colourful strong force vector bosons are seen in nature in isolation. While the non-zero frozen value of the propagator clearly has a scale it is strictly speaking not a true mass since that is adduced from a simple pole of a propagator. However, the key point from lattice data is that some scale can be associated with the infrared dynamics of the gluon. From a quantum field theory point of view understanding the origin of such a scale in a Lagrangian context could prove useful in gaining an insight into the colour confinement mechanism.

Over the years there have been various attempts at such an understanding. For instance, in [12] a gauge independent mass term for the gluon was considered. When quantum corrections were included this produced a gluon propagator whose full momentum dependence was remarkably consistent with the lattice data of recent years. Indeed the consequences of such an underlying gluon mass was explored in [13] where the glueball spectrum was constructed using a variational method approach. Another of the early and deep insights was provided by Gribov in [14]. There it was observed that the ambiguity deriving from the non-uniqueness of fixing the gauge globally could induce a cutoff in the path integral defining the gluon configuration space. Such a restriction affected the structure of the gluon propagator but in such a way as to retain its massless fundamental-like behaviour at high energy. However, taken in the full the propagator contained a new scale parameter called the Gribov mass and produced a positivity violating propagator, [14]. Though this new parameter was not an independent quantity as it satisfies a gap equation. In the current context the Gribov propagator suffered from the drawback that while freezing in the infrared to a finite value, that finite value was actually zero and not consistent with current lattice data. A modification [13, 14, 15, 16] of the Gribov construction built on Zwanziger's localization programme, [19, 20, 21, 22, 23, 24, 25, 26, 27, 28, 29], can be used to model the data. Moreover, that required the condensation of the additional localizing fields introduced in [16, 17, 18] to produce a dynamic mass scale aside from the Gribov mass which was already present. While successful in modelling the data it does not appear to be constructed in a fundamental way within the ethos of Gribov's elegant construction.

In recent years there has been a re-examination of the Gribov copy problem in a series of articles, [30, 31, 32]. For instance, in [30] a reweighting of the average of Gribov copies has produced a new Lagrangian in which to study Gribov copy issues and thence to examine their effect on the propagator at low momentum. In essence a new type of gauge fixed Lagrangian emerges with a new gauge parameter which has dimensions of mass. As an aside we note that like the work we have summarized so far we are concentrating throughout this article on the Landau gauge. This new gauge parameter is related to counting replicas derived from the Gribov copies, [30]. The resulting Lagrangian bears a strong resemblance to the nonlinear gauge known as the Curci-Ferrari gauge, [33, 34]. Moreover, it has similarities to earlier attempts to have a copy free gauge fixing such as those advocated in [35, 36, 37, 38]. In those articles a gluon mass term was added to the Lagrangian with the mass playing a role similar to a gauge parameter. The fixing was copy free since the additional term had the property of gauge invariance. Although, like the Gribov Lagrangian, the new Lagrangian was no longer local similar to the situation in [12]. More recently, the one loop analysis carried out for the propagators in [30] has been extended to one loop for vertex functions in three as well as four dimensions, [32]. While such propagator and vertex functions derived in [32] appear to be in general qualitative accord with lattice data, it is worth noting that parallel analyses using the Gribov-Zwanziger Lagrangian and its extensions also qualitatively agree with data. At this one loop precision it would be overambitious to hope for quantitative agreement. Instead one could aim to produce tests whereby certain Lagrangian motivated ansätze are excluded. For instance, in [39] the power corrections to the triple gluon vertex at one loop at the symmetric point had dimension two or four as the leading corrections depending on whether they were determined in a Gribov-Zwanziger or refined Gribov-Zwanziger Lagrangian compared with a gluon mass motivated model akin to [30, 31, 32]. Lattice data has not currently reached enough accuracy in the intermediate energy range where such power corrections can be differentiated between. Nevertheless it is worth pursuing this programme to higher loop order which is the purpose of this article.

Several additional comments are in order for balance to contrast the differing positions between the Gribov-Zwanziger approach and that of gluon mass model. By the latter we include both the original Curci-Ferrari model as well as the copy free observation of [30, 31, 32]. For instance, if one considers the energy-momentum tensor trace in the gluon mass case it is non-zero unlike the Gribov-Zwanziger situation. This is because the horizon condition defining the first Gribov region defines a gap equation for the Gribov mass which when imposed removes the non-zero contribution to the energy-momentum tensor trace. Such a gap equation derives naturally from the no pole condition of the Gribov construction which is not the case for a gluon mass model. Though in [40] it was argued that one could define a gap equation consistent with the renormalization group equation so that the mass was not a free parameter similar to the Gribov case. While such a condition is not fully similar to that of [30, 31, 32] it is indicative that a condition of some sort is required for such mass models. Another issue which is not unnatural to raise concerns whether the gluon propagator or correlator as measured on the lattice is actually the same quantity as is computed in a Lagrangian approach. Using field theories with explicit spin-1 mass terms could be regarded as merely modelling the lattice data. We include the refined Gribov-Zwanziger extension of [16, 17, 18] in these comments where localizing ghost mass is included. Thus there is no fully accepted explanation of the underlying mechanism behind a frozen gluon propagator. One point of view is that the loss of Lorentz symmetry using lattice regularization means it is difficult to be certain of true zero momentum behaviour in the restoration of the continuum limit. In a dimensional regularization translational invariance is not lost. Equally the zero momentum values of the gluon and Faddeev-Popov ghost propagators are not renormalization group invariants. So the specific value is not protected by that principle.

Instead an alternative position is that it could actually be the case that at low momentum the gluon propagator does indeed vanish analytically and the lattice definition of the spin-1 adjoint field in the infrared is not that of the continuum. As an aside while there is no symmetry principle as such which implies a vanishing gluon propagator, arguments have been given in [20, 41] that this is the case in the Gribov-Zwanziger Lagrangian. Currently, for the gluon this has been verified only at one loop and part of the motivation behind this article is actually to provide the computational algorithm for a future Gribov-Zwanziger analysis at two loops. Recently some evidence has been provided in [42] that the lattice gluon variables may not be the same as those of the continuum. To understand this we need to recall properties of the Gribov-Zwanziger formalism. In the pure case [14] the gluon propagator vanishes in the infrared with the Faddeev-Popov ghost propagator enhancing. The lattice finds a frozen gluon propagator and a non-enhanced Faddeev-Popov ghost propagator. The latter behaviour can be accommodated non-uniquely in the refined Gribov-Zwanziger scenario, [16, 17, 18]. However, in both scenarios there are predictions for the bosonic localizing ghost propagator. In the pure case it enhances like the Faddeev-Popov ghost which has been examined at one loop in [18, 43]. An all orders analysis was also provided in [41]. However, in the refined case at low momentum the bosonic localizing ghost propagator can either freeze to a non-zero value or behave in a non-enhanced way, [18]. The actual property depends on the different condensation channels. What has been interesting in the recent lattice study of the bosonic localizing ghost propagator of [42] is that an *enhanced* propagator emerges for it. In any Lagrangian analysis no such enhancement is present when the gluon propagator freezes to a non-zero finite value. Instead the vanishing of the gluon propagator at zero momentum is inextricably linked to the enhancement of its ghost partners. While [42] represents an early lattice investigation into the properties of this propagator it is perhaps premature to make a final statement on the difference in definition of gluon variables in various approaches.

Returning to our focus here we will extend the propagator analysis in the gluon mass model of [30] to two loops as the initial stage in providing more accurate tests. However, at this loop order this inevitably has to be in a limit since the underlying full two loop basic master Feynman integrals have yet to be determined as closed functions of mass for all values of momentum. Instead we will perform the analysis using a zero momentum expansion of the propagators within a Feynman integral. Such a computation is possible due to the algorithm developed in [44]. One aim is to refine the value of the propagator at zero mass. As discussed in [30] while the tree propagator of the model is similar to that of a scalar field the one loop corrections wash out the pole and produce a positivity violating propagator whose behaviour and shape is qualitatively in keeping with data, [30, 32]. Thus having a correction to the one loop freezing value of the gluon propagator in this model will aid the extraction of the fundamental scale that appears to be associated with the colour confinement picture. Although we have concentrated on the gluon a partner in the analysis is the Faddeev-Popov ghost. In the Gribov construction, [14], the ghost propagator was found to behave as a dipole propagator in the deep infrared. Hence it satisfied the Kugo-Ojima colour confinement criterion of [45, 46]. Indeed more recently, [47], this condition has been discussed in gauges other than Landau with indications that it may be pointing the way to understanding gluon confinement in a gauge independent fashion. Here we will also refine the two loop structure of the Faddeev-Popov ghost propagator and extend the computation of [32]. Such an approximate calculation of this and the gluon propagator will also serve as a useful independent check on any future *full* two loop analysis which is another motivation for the article.

The article is organized as follows. We provide the background quantum field theory to our computations in the next section including the essentials of the computational algorithm we will use. The results of its application to the four and three dimensional models are given in sections 3 and 4 respectively. Concluding remarks are given in section 5 while an appendix summarizes the expansion of several massive two loop propagator integrals.

2 Background.

We begin by recalling the key features of the gluon mass model, [30, 31, 32], in the Landau gauge which are required for the two loop analysis. The Lagrangian is [30, 31]

$$L ~=~ -~ \frac{1}{4} G^a_{\mu\nu} G^{a\,\mu\nu} ~+~ \frac{1}{2} m^2 A^a_\mu A^{a\,\mu} ~+~ \bar{c}^a \partial^\mu \left(D_\mu c \right)^a ~+~ i \bar{\psi} \not{D} \psi ~-~ \frac{1}{2\alpha} \left(\partial^\mu A^a_\mu \right)^2 \qquad (2.1)$$

where A^a_μ is the gluon field of mass m, c^a is the Faddeev-Popov ghost, ψ^i are the massless quarks and D_μ is the covariant derivative. While quarks essentially play a passive role in relation to the infrared behaviour we have included them here partly for completeness but also because of their value in internal checks within the automatic symbolic manipulations we will carry out. The index a runs over the range $1 \leq a \leq N_A$ where N_A is the dimension of the adjoint representation of the colour group. We have included the canonical gauge parameter α since a non-zero value is required to deduce the gluon propagator. Thereafter it is set to zero throughout as we will only be considering the Landau gauge. Thus in this gauge the A^a_μ propagator is

$$\langle A^a_\mu(p) A^b_\nu(-p) \rangle ~=~ - ~ \frac{\delta^{ab}}{[p^2+m^2]} \left[\eta_{\mu\nu} ~-~ \frac{p_\mu p_\nu}{p^2} \right] ~. \tag{2.2}$$

The Feynman rules for the remaining propagators are the same as those derived from the Lagrangian with m set to zero. As noted in [30] this mass parameter derives from a replica limit and the sampling of the Gribov copies in the gauge fixing. The idea being that the replica limit is taken before the Landau gauge limit and the presence of the mass should ensure that the deep infrared regime can be probed using perturbation theory, [30]. Indeed the analysis of [32] is not inconsistent with this proposal in relation to lattice data. As the early investigations into the use of (2.1) foundered on the loss of unitarity several comments are in order. For instance the Curci-Ferrari gauge and model have been examined on the lattice, [48, 49], as it is believed to circumvent the Neuberger problem. In those studies it is argued that for perturbative Green's functions the massless limit is smooth and that the appropriate way to take the limit is in a l'Hôpital sense. However, for (2.1) one should be careful in the point of view. Clearly the gluon propagator from (2.1) is of a fundamental form and as such it models lattice data. This does not imply that (2.1) represents the true position. Rather it should be regarded as an effective theory which is valid in some region. In other words it could be regarded as the leading form of an expansion of a more general but unitarity theory which is as yet not known. Indeed from our understanding of the Gribov construction it would not be unexpected if such a theory was non-local. So the arguments concerning the loss of unitarity of the Curci-Ferrari model which were applied to the theory as a whole may not be applicable in this effective situation.

Next we detail our method of computation. First, we generate the relevant one and two loop Feynman diagrams for the 2-point functions we are interested in using the QGRAF package, [50]. Overall there are 4 one loop and 23 two loop graphs for the gluon self energy. The respective numbers for the Faddeev-Popov ghost self energy are 1 and 7. In both cases these are larger than one would normally encounter in an analysis of the structure of 2-point functions in QCD because one has to allow for massive snail graphs deriving from the closure of two legs on a quartic gluon vertex. Ordinarily such a graph would be zero in massless QCD. The electronic representations of the graphs are then converted into FORM input notation where FORM is a symbolic manipulation language, [51]. At this stage the Lorentz, colour and spinor indices are appended. As we are interested in the zero momentum behaviour of the 2-point functions we cannot use the vacuum bubble expansion of [52, 53]. This is because this is primarily to determine the divergent parts of the contributing Feynman graphs in order to deduce the corresponding renormalization group functions. In other words the vacuum bubble expansion is an automatic way of implementing the method of infrared rearrangement, [52, 53]. Instead we use the method of [44] which is a way of determining the correct finite part of basic Feynman integrals when one is expanding at low momentum. This is a non-trivial task as emphasised in [44]. The main reason for this is that if one naively expanded an integral in powers of momentum, for certain integrals with massless propagators one would obtain spurious infrared divergences. Moreover, if not handled systematically by some technique one could be led to obtain results which would contradict the renormalizability of the underlying quantum field theory. Given these general observations in [44], where a robust method of expansion of such Feynman integrals was provided, the relevant parts of [44] will be discussed later. However, in order to be able to apply such a technique we first have to write the contributing Feynman integrals for each graph in a compact notation.

In choosing to follow [44] we concentrate for the most part on the two loop situation as the process for one loop graphs is similar but considerably simpler. We define the general two loop self-energy integral by

$$\begin{aligned} & I_{m_1 m_2 m_3 m_4 m_5}(n_1, n_2, n_3, n_4, n_5) \\ &= \int_{kl} \frac{1}{[k^2+m_1^2]^{n_1}[l^2+m_2^2]^{n_2}[(k-p)^2+m_3^2]^{n_3}[(l-p)^2+m_4^2]^{n_4}[(k-l)^2+m_5^2]^{n_5}} \end{aligned} \quad (2.3)$$

where $\int_k = \int d^dk/(2\pi)^d$ and d is the space-time dimension. Our notation is similar to [44] but we note that the order of our labels differs from that of [44]. Also for the specific problem we are interested in $m_i \in \{0, m\}$. Given the structure of this general two loop 2-point function, it is possible to write, using a FORM module, all numerator scalar products of the three different momenta in terms of the denominator factors. In other words there are no irreducible tensors for (2.3). At this stage there are several ways of extracting the low momentum behaviour. For instance, one could apply the method of [44] directly to each of the contributing integrals but regard this as inefficient. Instead we have chosen to apply the Laporta algorithm, [54]. This is a technique to create integration by parts identities between all the necessary integrals and then solve them order by order from a level which includes the highest numerator power. The method then produces a series of relations between all the integrals required for the full calculation and a relatively small set of base integrals which are known as the masters, [54]. The expressions for these can be substituted when they are evaluated by methods other than integration by parts. In our particular case not all the two loop self energy master integrals are known for all mass configurations. For instance, some are available for cases which are relevant to standard model analyses, [55]. Therefore at this stage we substitute the values for each master integral from the values obtained from applying the method of [44] to the emerging master integrals. In order to apply the Laporta algorithm we have chosen to use the REDUZE implementation, [56], which uses GiNaC, [57], and is written in C++. Once the setup parameters are specified for the basic topologies and mass configuration, REDUZE creates a database. From this we can extract the relations for all the integrals relevant to the self-energy analysis in terms of the master integrals. Again we use the feature of REDUZE that allows for the output from the database to be written as a FORM module. Therefore, we can perform the full computation for each of the 2-point functions of interest automatically. Moreover, we have carried this out in such a way that the three dimensional analysis can also be performed. This requires constructing a separate FORM module for substituting the three dimensional master integrals.

The next stage is the insertion of the low momentum expansion of the emergent master integrals. These can be classified into several sets dependent upon the number of propagators. In some cases the exact expression for such masters is known which is the case for two and three propagator two loop self energy integrals. We note that the Laporta algorithm [54] is designed in such a way that only non-trivial masters arise. For instance, those integrals which are zero because of a massless one loop bubble never emerge in the REDUZE output. So one two loop two propagator case is the product of two one loop massive vacuum bubbles. Equally the three propagator case can be the basic sunset topology with different mass configurations, or the product of a one loop massless or massive self energy graph with a one loop massive vacuum bubble. In these cases the low momentum values are trivial to substitute. Though we note that in certain cases the Laporta algorithm may produce a sunset topology with an irreducible numerator. For this and the four and five propagator cases we resort to the algorithm of [44] which we briefly recall.

In general, integrals such as (2.3) can be expanded in powers of p^2/m^2 where p is the external momentum. However, as noted in [44] the naive expansion of the constituent propagators within the integral itself does not necessarily lead to the correct expansion. This is straightforward to see in a simple example. As is well known $I_{m0000}(1,1,1,1,1)$ is a finite integral and its exact value is known [55]. However, if one naively Taylor expands a massless propagator within $I_{m0000}(1,1,1,1,1)$ which depends on the external momentum p, then the terms of the Taylor series in p beyond the leading one, when finally evaluated witin the context of the overall Feynman integral itself will have poles in ϵ. These divergences are infrared in nature since the overall original Feynman integral was infrared finite. They arise due to the simple fact that expanding a p dependent massless propagator, which is not protected by a non-zero mass, will naturally produce propagators which have infrared singularities. Hence this expansion approach cannot be used. However, in [44] a method was developed where these infrared singularities could be systematically cancelled. It relies on understanding the particle thresholds within the basic graph when various mass configurations are present. Clearly if a p dependent propagator has a non-zero mass then Taylor expanding it in the usual way does not introduce any infrared singularities. The problem arises in (2.3) when it is not possible to route the external momentum through the propagators from one external vertex to the other via a full set of *massive* propagators. An example of when this is not possible is when one of the one loop subgraphs of (2.3) is completely massless. In this and other instances, [44] provided an algorithm where the naive expansion of the propagators in (2.3) have the expansion of related but different integrals appended. Symbolically this is given by

$$I_\Gamma ~\sim~ \sum_\lambda I_{\Gamma/\lambda} \circ \mathcal{T}_{\{q_i\}} I_\lambda \tag{2.4}$$

where I_Γ corresponds to the integral of (2.3), Γ corresponds to the original graph and γ is a subgraph of Γ. The sum is over a particular set of subgraphs. This is the set of subgraphs which contain all the massive propagators and are one particle irreducible with respect to the massless lines, [44]. The graph corresponding to Γ/γ is that where the subgraph γ has been shrunk to a point. Finally, within the sum the integral corresponding to the subgraph is first expanded using the $\mathcal{T}_{\{q_i\}}$ operator, where q_i are a particular set of momenta of the subgraph γ, and which operates on the propagators. The specific set $\{q_i\}$ depends in the mass configuration of the original Feynman integral. For instance, [44],

$$T_l \frac{1}{[(l-p)^2+m_4^2]} ~=~ \sum_{i=0}^\infty \frac{[2lp-l^2]^i}{[l^2+m_4^2]^{i+1}} \tag{2.5}$$

where m_4 does not have to be non-zero here. Once the expansion of all the subgraphs has been carried out to the necessary order for the overall 2-point functions of the problem at hand, the integration over the two loop momenta of the integral of the master is performed. The individual integrals which emerge to complete the determination of each master are either two loop massive vacuum bubbles, the product of one loop integrals or massless two loop integrals. At this stage we have chosen to build a second REDUZE database in order to handle the reduction of the first of these three classes down to a base set of two loop master vacuum bubbles. The explicit expressions for these have been known for a long time for four dimensions. For example, see [58, 59, 60], for four dimensions and [61] for three dimensions. Once the expansions have been obtained they are substituted at the appropriate point of the overall automatic FORM computation. We note that in developing this FORM module we have checked the expansion algorithm we have written for the known cases given in [44] in four dimensions and find agreement. As a final check on the overall expansion, when all the diagrams contributing to a 2-point function are summed we recover the usual $\overline{\mathrm{MS}}$ renormalization constants for the gluon and quark wave function renormalizations as well as that for the gluon mass parameter in the Landau gauge. This ensures that no rogue infrared divergence from the application of the algorithm of [44] to the masters has survived to upset the renormalizability of QCD.

3 Four dimensions.

In this section we collect the results for the low momentum expansion of the propagators in four dimensions. As a check on the computation we have recovered the correct $\overline{\text{MS}}$ divergences in the Landau gauge in the presence of a gluon mass term. This is a non-trivial check on the computation since we are evaluating massive Feynman diagrams in a zero momentum limit. Therefore, we have to be sure that using the approach of [44] we do not incorrectly include an infrared divergence in dimensional regularization as it is indistinguishable from an ultraviolet one. For instance, a mismatch in the application of the diagram subtraction process of [44] could produce such a pole in ϵ. Therefore, we note that in the four dimensional case we have correctly obtained the known two loop $\overline{\text{MS}}$ wave function renormalization constants for the gluon and the ghost, [62, 63], as well as the Slavnov-Taylor identity for the gluon mass term. As was originally noted in [64] and subsequently rediscovered in a three loop computation in [65], the anomalous dimension of m satisfies

$$\gamma_m(a) \;=\; \frac{1}{2}\left[\gamma_A(a) \;+\; \gamma_c(a)\right] \tag{3.1}$$

in the Landau gauge where $\gamma_i(a)$ is the anomalous dimension of the quantity i, $a = g^2/(16\pi^2)$ and g is the coupling constant. We note that (3.1) differs by a factor of 2 from the relation presented in [65]. This is because in [65] the anomalous dimension of the gluon mass operator itself was determined and the renormalization constant of the mass operator and the mass parameter, m, are not equivalent but related by a power. For clarity we note that we renormalize the gluon mass with

$$m_{\mathrm{o}} \;=\; Z_m\, m \tag{3.2}$$

where $_{\mathrm{o}}$ indicates a bare quantity, and $\gamma_m(a)$ is the anomalous dimension associated with the gluon mass renormalization constant Z_m.

Applying the algorithm we have outlined earlier to the gluon and ghost 2-point functions we find that at low momentum the former is

$$\begin{aligned}
\langle A^a_\mu(p) A^b_\nu(-p)\rangle \;=\; & \Bigg[- p^2 - m^2 \\
& + \Bigg[\left[- \frac{5}{8} + \frac{3}{4} \ln\left(\frac{m^2}{\mu^2}\right) \right] m^2 C_A \\
& \quad + \left[- \frac{1}{8} - \frac{25}{12} \ln\left(\frac{m^2}{\mu^2}\right) - \frac{1}{12} \ln\left(\frac{p^2}{\mu^2}\right) \right] p^2 C_A \\
& \quad + \left[- \frac{20}{9} + \frac{4}{3} \ln\left(\frac{p^2}{\mu^2}\right) \right] p^2 T_F N_f \Bigg] a \\
& + \Bigg[\left[\frac{743}{384} - \frac{891}{128} s_2 + \frac{11}{64} \zeta(2) + \frac{245}{96} \ln\left(\frac{m^2}{\mu^2}\right) - \frac{53}{32} \ln^2\left(\frac{m^2}{\mu^2}\right) \right] m^2 C_A^2 \\
& \quad + \left[\frac{5}{24} + \zeta(2) - \frac{2}{3} \ln\left(\frac{m^2}{\mu^2}\right) + \frac{1}{2} \ln^2\left(\frac{m^2}{\mu^2}\right) \right] m^2 T_F C_A N_f \\
& \quad + \Bigg[- \frac{737}{216} + \frac{45}{8} s_2 - \frac{2}{9} \zeta(2) - \frac{145}{144} \ln\left(\frac{m^2}{\mu^2}\right) + \frac{3}{2} \ln^2\left(\frac{m^2}{\mu^2}\right) \\
& \qquad + \frac{1}{8} \ln\left(\frac{m^2}{\mu^2}\right) \ln\left(\frac{p^2}{\mu^2}\right) - \frac{5}{48} \ln\left(\frac{p^2}{\mu^2}\right) \Bigg] p^2 C_A^2 \\
& \quad + \Bigg[- \frac{139}{108} + 2\zeta(2) + \frac{35}{9} \ln\left(\frac{m^2}{\mu^2}\right) + \ln^2\left(\frac{m^2}{\mu^2}\right)
\end{aligned}$$

$$
\begin{aligned}
& - \; 2\ln\left(\frac{m^2}{\mu^2}\right)\ln\left(\frac{p^2}{\mu^2}\right) + \frac{5}{3}\ln\left(\frac{p^2}{\mu^2}\right)\Bigg] p^2 T_F C_A N_f \\
& + \left[- \; 3 + 4\ln\left(\frac{m^2}{\mu^2}\right)\right] p^2 T_F C_F N_f \Bigg] a^2 \; + \; O\left(a^3; (p^2)^3\right) \Bigg] P_{\mu\nu}(p) \\
+ \Big[- \; m^2 & \\
& + \left[\left[- \; \frac{5}{8} + \frac{3}{4}\ln\left(\frac{m^2}{\mu^2}\right)\right] m^2 C_A + \left[\frac{11}{24} - \frac{1}{4}\ln\left(\frac{p^2}{m^2}\right)\right] p^2 C_A\right] a \\
& + \Bigg[\Bigg[\frac{743}{384} - \frac{891}{128}s_2 + \frac{11}{64}\zeta(2) + \frac{245}{96}\ln\left(\frac{m^2}{\mu^2}\right) - \frac{53}{32}\ln^2\left(\frac{m^2}{\mu^2}\right)\Bigg] m^2 C_A^2 \\
& + \left[\frac{5}{24} + \zeta(2) - \frac{2}{3}\ln\left(\frac{m^2}{\mu^2}\right) + \frac{1}{2}\ln^2\left(\frac{m^2}{\mu^2}\right)\right] m^2 T_F C_A N_f \\
& + \Bigg[\frac{4967}{1152} - \frac{459}{32}s_2 - \frac{5}{24}\zeta(2) - \frac{53}{48}\ln\left(\frac{m^2}{\mu^2}\right) + \frac{3}{8}\ln\left(\frac{m^2}{\mu^2}\right)\ln\left(\frac{p^2}{m^2}\right) \\
& - \; \frac{5}{16}\ln\left(\frac{p^2}{\mu^2}\right)\Bigg] p^2 C_A^2 + \left[- \; \frac{5}{9} + \frac{1}{3}\ln\left(\frac{m^2}{\mu^2}\right)\right] p^2 T_F C_A N_f \Bigg] a^2 \\
& + \; O\left(a^3; (p^2)^3\right)\Big] L_{\mu\nu}(p)
\end{aligned}
\tag{3.3}
$$

where

$$
P_{\mu\nu}(p) \; = \; \eta_{\mu\nu} \; - \; \frac{p_\mu p_\nu}{p^2} \quad , \quad L_{\mu\nu}(p) \; = \; \frac{p_\mu p_\nu}{p^2}
\tag{3.4}
$$

$\zeta(z)$ is the Riemann zeta function, $s_2 = (2\sqrt{3}/9)\mathrm{Cl}_2(2\pi/3)$ which involves the Clausen function $\mathrm{Cl}_2(\theta)$, and μ is the renormalization scale introduced as a consequence of the dimensional regularization in order to handle the dimensionality of the coupling constant in d-dimensions. Numerically $s_2 = 0.2604341$. The order symbols are intended to indicate the order in which each of the coupling constant and momentum powers the expansion is performed to. The colour group Casimirs C_A, C_F and T_F are given by

$$
T^a T^a \; = \; C_F I \quad , \quad f^{acd} f^{bcd} \; = \; C_A \delta^{ab} \quad , \quad \mathrm{Tr}\left(T^a T^b\right) \; = \; T_F \delta^{ab}
\tag{3.5}
$$

where T^a are the generators of the colour group whose structure constants are f^{abc}, I is the unit matrix which with T^a complete the basis for colour space. To appreciate the relative properties of the loop corrections we have plotted the coefficient of $(-1)m^2 a^L$ at zero momentum for $N_f = 3$ where $L = 0$, 1 and 2 in Figure 1 where $x = m^2/\mu^2$. For low values of x the corrections have the same signs.

The situation for the ghost is somewhat similar though simpler since

$$
\begin{aligned}
\langle c^a(p)\bar{c}^b(-p)\rangle \; = \; & \Bigg[- \; 1 + \left[\frac{5}{8} - \frac{3}{4}\ln\left(\frac{m^2}{\mu^2}\right)\right] C_A a \\
& + \Bigg[\Bigg[- \; \frac{893}{384} + \frac{891}{128}s_2 - \frac{11}{64}\zeta(2) - \frac{155}{96}\ln\left(\frac{m^2}{\mu^2}\right) + \frac{35}{32}\ln^2\left(\frac{m^2}{\mu^2}\right)\Bigg] C_A^2 \\
& + \left[- \; \frac{5}{24} - \zeta(2) + \frac{2}{3}\ln\left(\frac{m^2}{\mu^2}\right) - \frac{1}{2}\ln^2\left(\frac{m^2}{\mu^2}\right)\right] T_F C_A N_f \Bigg] a^2 \\
& + \; O(a^3)\Bigg] p^2 \; + \; O\left((p^2)^2\right) \; .
\end{aligned}
\tag{3.6}
$$

One interesting feature of both 2-point functions resides in the one loop leading order terms which are very similar. For instance, if we were in a Gribov scenario then there is a gap equation for

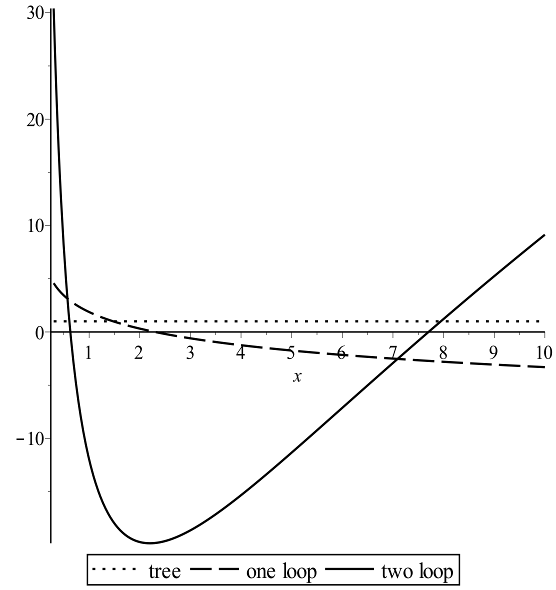

Figure 1: Plots of the leading term, one loop and two loop coefficients of $(-1)m^2$ in the four dimensional zero momentum gluon propagator for $N_f = 3$.

the corresponding mass parameter deriving from the horizon condition defining the boundary of the first Gribov region, [14]. This condition when imposed means that the ghost propagator enhances and, moreover, satisfies the Kugo-Ojima confinement criterion, [45, 46]. However, if one wished to impose a Kugo-Ojima type confinement criterion on the Faddeev-Popov ghost propagator in order to have ghost enhancement it might appear that at the same stroke the gluon propagator would be massless at zero momentum. A closer examination of the actual signs clearly indicates, however, that such a scenario does not occur. Setting such a pseudo-Kugo-Ojima criterion, for example, merely retains a non-zero value for the gluon propagator at zero momentum or in other words a frozen propagator consistent with the decoupling scenario, [10, 11], favoured by lattice data, [1, 2, 3, 4, 5, 6, 7, 8, 9]. The Faddeev-Popov ghost would then enhance but this is not observed in lattice data when there is a non-zero frozen gluon propagator.

4 Three dimensions.

We have repeated the analysis for the three dimensional case. The procedure is the same with the main difference being the use of different master integrals after the application of the Laporta reduction. Therefore, we have adapted our FORM code to accommodate this variation. However, there are some novel features in three dimensions compared with the previous section. For instance, the theory is superrenormalizable and hence not every Green's function is divergent. It transpires that to two loops both the gluon and ghost 2-point functions are finite when there is a non-zero gluon mass term in the Lagrangian. Therefore unlike the four dimensional case when the divergences for these Green's functions are known and thereby provide an internal check on the computations, there is no such check in this case. However, the use of predominantly the same code aside from master integrals should ensure the correctness of our results in this instance. Another aspect of the superrenormalizability relates to the dimensionality of the coupling constant which is no longer dimensionless. Instead in three dimensions a has mass dimension one. One point which may arise concerning the applicability of the approach to the three dimensional case relates to the work of [66]. In [66] massless gauge theories were examined at two loops due to the potential breakdown of perturbation theory. However, it was shown that this was not the case. Here the corresponding situation does not arise since the presence of the mass obviates this issue.

For the gluon 2-point function we find that to two loops the low momentum structure is

$$
\begin{aligned}
\langle A^a_\mu(p) A^b_\nu(-p) \rangle &= \Bigg[- p^2 - m^2 + \left[\frac{1}{64} \sqrt{p^2} C_A - \frac{1}{8} \sqrt{p^2} T_F N_f - \frac{1}{6\pi} m C_A + \frac{9}{40\pi} \frac{p^2}{m} C_A \right] a \\
&\quad + \Bigg[\frac{1}{192\pi} \frac{\sqrt{p^2}}{m} C_A^2 - \frac{1}{24\pi} \frac{\sqrt{p^2}}{m} C_A T_F N_f \\
&\qquad + \left[- \frac{121}{1536} - \frac{1}{12} \ln(2) + \frac{21}{256} \ln(3) \right] \frac{C_A^2}{\pi^2} + \frac{1}{48\pi^2} C_A T_F N_f \\
&\qquad + \left[- \frac{11951}{691200} + \frac{9}{1280} \ln(3) + \frac{1}{1280} \ln \left(\frac{p^2}{m^2} \right) \right] \frac{p^2}{m^2} \frac{C_A^2}{\pi^2} - \frac{1}{16384} \frac{p^2}{m^2} C_A^2 \\
&\qquad + \left[\frac{139}{1800\pi^2} - \frac{1}{80\pi^2} \ln \left(\frac{p^2}{m^2} \right) \right] \frac{p^2}{m^2} C_A T_F N_f - \frac{1}{512} \frac{p^2}{m^2} C_A T_F N_f \\
&\qquad - \frac{1}{16\pi^2} \frac{p^2}{m^2} C_F T_F N_f + \frac{1}{256} \frac{p^2}{m^2} C_F T_F N_f \Bigg] a^2 ~+~ O \left(a^3 ; (p^2)^{\frac{3}{2}} \right) \Bigg] P_{\mu\nu}(p) \\
&+ \Bigg[- m^2 + \left[\frac{1}{32} \sqrt{p^2} C_A - \frac{1}{6\pi} m C_A - \frac{1}{30\pi} \frac{p^2}{m} C_A \right] a \\
&\quad + \Bigg[\frac{1}{96\pi} \frac{\sqrt{p^2}}{m} C_A^2 + \left[- \frac{121}{1536} - \frac{1}{12} \ln(2) + \frac{21}{256} \ln(3) \right] \frac{C_A^2}{\pi^2} + \frac{1}{48\pi^2} C_A T_F N_f \\
&\qquad + \left[- \frac{1783}{115200} - \frac{5}{96} \ln(2) + \frac{13}{320} \ln(3) + \frac{1}{960} \ln \left(\frac{p^2}{m^2} \right) \right] \frac{p^2}{m^2} \frac{C_A^2}{\pi^2} \\
&\qquad - \frac{3}{4096} \frac{p^2}{m^2} C_A^2 + \left[- \frac{31}{3600\pi^2} + \frac{1}{240\pi^2} \ln \left(\frac{p^2}{m^2} \right) \right] \frac{p^2}{m^2} C_A T_F N_f \Bigg] a^2 \\
&+ O \left(a^3 ; (p^2)^{\frac{3}{2}} \right) \Bigg] L_{\mu\nu}(p) ~.
\end{aligned}
\tag{4.1}
$$

In terms of structure for these corrections compared to the four dimensional case the role s_2 played is taken now by the presence of $\ln(2)$ and $\ln(3)$. For the ghost 2-point function the situation is somewhat simpler since

$$
\begin{aligned}
\langle c^a(p) \bar{c}^b(-p) \rangle &= \Bigg[- 1 + \frac{C_A}{6\pi m} a \\
&\quad + \left[\left[\frac{235}{4608} + \frac{1}{12} \ln(2) - \frac{21}{256} \ln(3) \right] \frac{C_A^2}{\pi^2 m^2} - \frac{1}{48} \frac{C_A T_F N_f}{\pi^2 m^2} \right] a^2 ~+~ O(a^3) \Bigg] p^2 \\
&+ O \left((p^2)^2 \right) ~.
\end{aligned}
\tag{4.2}
$$

Moreover, we observe that there is a similar structure to the four dimensional case. Within the one loop ghost 2-point function one can observe the origins of the Gribov mass gap equation and the same comments apply in relation to what was stated for the Kugo-Ojima criterion earlier. Equally the situation is blurred at two loops since the mixed mass scale master integrals can not be adduced within the above results.

5 Discussion.

We conclude with brief remarks. In analysing the two loop corrections to the gluon and ghost propagators in this effective theory of Gribov copies, [30, 31, 32], we have provided useful values for the approach to zero momentum. This will be important for the programme proposed in [31] which indicated that the exact evaluation of the two loop corrections would be possible. For instance, having *independent* computations, albeit in the low momentum limit, is crucial to establishing the correctness of an exact result. However, the determination of the two loop correction to where the gluon propagator freezes emerges from this calculation. Indeed there are intriguing similarities to the structure of the corrections when compared to propagators evaluated in the Gribov-Zwanziger construction. For instance, a pseudo-mass gap appears to be present which is similar in terms of numerical values to the gap equation for the Gribov mass.

Acknowledgements. The author thanks Dr M. Tissier for useful discussions.

A Master integrals.

In this appendix we give the ϵ expansion for several master integrals which were required in three and four dimensions. We have applied the method of [44] and have reproduced the expressions given for the various integrals in Table 1 of [44]. As the REDUZE algorithm produces additional master integrals for our particular computation we note that several of these are

$$
\begin{aligned}
I_{m0m00}(1,1,1,0,1) &= \frac{1}{2\epsilon^2} + \left[\frac{1}{2} - \ln\left(\frac{m^2}{\mu^2}\right)\right]\frac{1}{\epsilon} + \frac{1}{2} - \ln\left(\frac{m^2}{\mu^2}\right) + \ln^2\left(\frac{m^2}{\mu^2}\right) + \frac{3}{2}\zeta(2) \\
&+ \left[-\frac{1}{6\epsilon} - \frac{1}{3} + \frac{1}{3}\ln\left(\frac{m^2}{\mu^2}\right)\right]\frac{p^2}{m^2} \\
&+ \left[\frac{1}{60\epsilon} + \frac{11}{120} - \frac{1}{30}\ln\left(\frac{m^2}{\mu^2}\right)\right]\frac{(p^2)^2}{m^4} \\
&+ \left[-\frac{1}{420\epsilon} - \frac{1}{45} + \frac{1}{210}\ln\left(\frac{m^2}{\mu^2}\right)\right]\frac{(p^2)^3}{m^6} + O\left(\frac{(p^2)^4}{m^8}\right) \\
I_{mm00m}(1,1,1,0,1) &= \frac{1}{2\epsilon^2} + \left[\frac{3}{2} - \ln\left(\frac{m^2}{\mu^2}\right)\right]\frac{1}{\epsilon} + \frac{7}{2} - \frac{27}{2}s_2 - 3\ln\left(\frac{m^2}{\mu^2}\right) + \ln^2\left(\frac{m^2}{\mu^2}\right) \\
&+ \frac{1}{2}\zeta(2) + \left[-\frac{1}{2\epsilon} - \frac{3}{4} + \ln\left(\frac{m^2}{\mu^2}\right)\right]\frac{p^2}{m^2} \\
&+ \left[\frac{1}{6\epsilon} + \frac{1}{2} - \frac{1}{3}\ln\left(\frac{m^2}{\mu^2}\right)\right]\frac{(p^2)^2}{m^4} \\
&+ \left[-\frac{1}{12\epsilon} - \frac{113}{360} + \frac{1}{6}\ln\left(\frac{m^2}{\mu^2}\right)\right]\frac{(p^2)^3}{m^6} + O\left(\frac{(p^2)^4}{m^8}\right) \\
I_{mmm0m}(1,1,1,0,1) &= \frac{1}{2\epsilon^2} + \left[\frac{1}{2} - \ln\left(\frac{m^2}{\mu^2}\right)\right]\frac{1}{\epsilon} + \frac{1}{2} - \frac{9}{2}s_2 - \ln\left(\frac{m^2}{\mu^2}\right) + \ln^2\left(\frac{m^2}{\mu^2}\right) + \frac{1}{2}\zeta(2) \\
&+ \left[-\frac{1}{6\epsilon} - \frac{2}{9} + s_2 + \frac{1}{3}\ln\left(\frac{m^2}{\mu^2}\right)\right]\frac{p^2}{m^2}
\end{aligned}
$$

$$
\begin{aligned}
&+\left[\frac{1}{60\epsilon}+\frac{247}{3240}-\frac{2}{9}s_2-\frac{1}{30}\ln\left(\frac{m^2}{\mu^2}\right)\right]\frac{(p^2)^2}{m^4}\\
&+\left[-\frac{1}{420\epsilon}-\frac{113}{4860}+\frac{2}{27}s_2+\frac{1}{210}\ln\left(\frac{m^2}{\mu^2}\right)\right]\frac{(p^2)^3}{m^6} \;+\; O\left(\frac{(p^2)^4}{m^8}\right)
\end{aligned}
$$

$$
\begin{aligned}
I_{mm00m}(1,1,1,1,1) &= \left[\frac{27}{2}s_2-\zeta(2)-\left[\frac{3}{2}+\frac{27}{4}s_2-\frac{3}{2}\zeta(2)\right]\frac{p^2}{m^2}+\left[\frac{47}{18}-\frac{4}{3}\zeta(2)\right]\frac{(p^2)^2}{m^4}\right.\\
&\quad\left.-\left[\frac{1703}{720}-\frac{27}{8}s_2-\frac{3}{4}\zeta(2)\right]\frac{(p^2)^3}{m^6}\right]\frac{1}{m^2} \;+\; O\left(\frac{(p^2)^4}{m^{10}}\right)\\
I_{mmmmm}(1,1,1,1,1) &= \left[3s_2-\left[\frac{2}{27}+\frac{1}{6}s_2\right]\frac{p^2}{m^2}+\left[\frac{29}{972}-\frac{1}{27}s_2\right]\frac{(p^2)^2}{m^4}\right.\\
&\quad\left.-\left[\frac{367}{29160}-\frac{11}{324}s_2\right]\frac{(p^2)^3}{m^6}\right]\frac{1}{m^2} \;+\; O\left(\frac{(p^2)^4}{m^{10}}\right) \qquad \text{(A.1)}
\end{aligned}
$$

in four dimensions.

In three dimensions similar masters are required but in contrast to four dimensions they do not have poles in ϵ. For comparison we record the same masters are

$$
\begin{aligned}
I_{m0m00}(1,1,1,0,1) &= \left[\frac{1}{32}-\frac{5}{576}\frac{p^2}{m^2}+\frac{1}{300}\frac{(p^2)^2}{m^4}-\frac{151}{94080}\frac{(p^2)^3}{m^6}\right]\frac{1}{\pi^2 m^2}\\
&\quad+O\left(\frac{(p^2)^4}{m^{10}}\right)\\
I_{mm00m}(1,1,1,0,1) &= \left[-\frac{1}{16}\ln\left(\frac{2}{3}\right)+\left[-\frac{1}{384}+\frac{1}{48}\ln\left(\frac{2}{3}\right)\right]\frac{p^2}{m^2}\right.\\
&\quad+\left[\frac{9}{5120}-\frac{1}{80}\ln\left(\frac{2}{3}\right)\right]\frac{(p^2)^2}{m^4}\\
&\quad\left.+\left[-\frac{55}{43008}+\frac{1}{112}\ln\left(\frac{2}{3}\right)\right]\frac{(p^2)^3}{m^6}\right]\frac{1}{\pi^2 m^2} \;+\; O\left(\frac{(p^2)^4}{m^{10}}\right)\\
I_{mmm0m}(1,1,1,0,1) &= \left[\frac{1}{96}-\frac{5}{3888}\frac{p^2}{m^2}+\frac{323}{1555200}\frac{(p^2)^2}{m^4}-\frac{20789}{548674560}\frac{(p^2)^3}{m^6}\right]\frac{1}{\pi^2 m^2}\\
&\quad+O\left(\frac{(p^2)^4}{m^{10}}\right)\\
I_{mm00m}(1,1,1,1,1) &= \left[\frac{1}{16}\ln\left(\frac{4}{3}\right)+\left[\frac{1}{192}-\frac{1}{12}\ln\left(\frac{4}{3}\right)\right]\frac{p^2}{m^2}\right.\\
&\quad+\left[\frac{13}{7680}+\frac{13}{240}\ln\left(\frac{4}{3}\right)\right]\frac{(p^2)^2}{m^4}\\
&\quad\left.+\left[-\frac{1531}{107520}-\frac{1}{210}\ln\left(\frac{4}{3}\right)\right]\frac{(p^2)^3}{m^6}\right]\frac{1}{\pi^2 m^4}\\
&\quad+O\left(\frac{(p^2)^4}{m^{12}}\right)\\
I_{mmmmm}(1,1,1,1,1) &= \left[\frac{1}{576}-\frac{1}{1944}\frac{p^2}{m^2}+\frac{1451}{11197440}\frac{(p^2)^2}{m^4}-\frac{2941}{94058496}\frac{(p^2)^3}{m^6}\right]\frac{1}{\pi^2 m^4}\\
&\quad+O\left(\frac{(p^2)^4}{m^{12}}\right)\;. \qquad \text{(A.2)}
\end{aligned}
$$

The expressions for the four dimensional case should be useful for other problems.

References.

[1] A. Cucchieri & T. Mendes, PoS LAT2007 (2007), 297.

[2] I.L. Bogolubsky, E.M. Ilgenfritz, M. Müller-Preussker & A. Sternbeck, PoS LAT2007 (2007), 290.

[3] A. Maas, Phys. Rev. **D75** (2007), 116004.

[4] A. Sternbeck, L. von Smekal, D.B. Leinweber & A.G. Williams, PoS LAT2007 (2007), 304.

[5] I.L. Bogolubsky, E.M. Ilgenfritz, M. Müller-Preussker & A. Sternbeck, Phys. Lett. **B676** (2009), 69.

[6] A. Cucchieri & T. Mendes, Phys. Rev. Lett. **100** (2008), 241601.

[7] A. Cucchieri & T. Mendes, Phys. Rev. **D78** (2008), 094503.

[8] O. Oliveira & P.J. Silva, Phys. Rev. **D79** (2009), 031501.

[9] Ph. Boucaud, J.P. Leroy, A.L. Yaounac, J. Micheli, O. Pène & J. Rodríguez-Quintero, JHEP **0806** (2008), 099.

[10] A.C. Aguilar, D. Binosi & J. Papavassiliou, Phys. Rev. **D78** (2008), 025010.

[11] C.S. Fischer, A. Maas & J.M. Pawlowski, Annals Phys. **324** (2009), 2408.

[12] J.M. Cornwall, Phys. Rev. **D26** (1982), 1453.

[13] J.M. Cornwall & A. Soni, Phys. Lett. **B120** (1983), 431.

[14] V.N. Gribov, Nucl. Phys. **B139** (1978), 1.

[15] D. Dudal, S.P. Sorella, N. Vandersickel & H. Verschelde, Phys. Rev. **D77** (2008), 071501.

[16] D. Dudal, J.A. Gracey, S.P. Sorella, N. Vandersickel & H. Verschelde, Phys. Rev. **D78** (2008), 065047.

[17] D. Dudal, J.A. Gracey, S.P. Sorella, N. Vandersickel & H. Verschelde, Phys. Rev. **D78** (2008), 125012.

[18] J.A. Gracey, Phys. Rev. **D82** (2010), 085032.

[19] D. Zwanziger, Nucl. Phys. **B209** (1982), 336.

[20] D. Zwanziger, Nucl. Phys. **B321** (1989), 591.

[21] D. Zwanziger, Nucl. Phys. **B323** (1989), 513.

[22] G. Dell'Antonio & D. Zwanziger, Nucl. Phys. **B326** (1989), 333.

[23] G. Dell'Antonio & D. Zwanziger, Commun. Math. Phys. **138** (1991), 291.

[24] D. Zwanziger, Nucl. Phys. **B364** (1991), 127.

[25] D. Zwanziger, Nucl. Phys. **B378** (1992), 525.

[26] D. Zwanziger, Nucl. Phys. **B399** (1993), 477.

[27] D. Zwanziger, Nucl. Phys. **B412** (1994), 657.

[28] D. Zwanziger, Phys. Rev. **D65** (2002), 094039.

[29] D. Zwanziger, Phys. Rev. **D69** (2004), 016002.

[30] J. Serreau & M. Tissier, Phys. Lett. **B712** (2012), 97.

[31] J. Serreau, M. Tissier & A. Tresmontant, Phys. Rev. **D89** (2014), 125019.

[32] M. Pelaez, M. Tissier & N. Wschebor, Phys. Rev. **D88** (2013), 125003.

[33] G. Curci & R. Ferrari, Nuovo Cim. **A32** (1976), 151.

[34] R. Delbourgo & P.D. Jarvis, J. Phys. **A15** (1982), 611.

[35] D. Zwanziger, Nucl. Phys. **B345** (1990), 461.

[36] C. Parrinello & G. Jona-Lasinio, Phys. Lett. **B251** (1990), 175.

[37] S. Fachin & C. Parrinello, Phys. Rev. **D44** (1991), 2558.

[38] S. Fachin, Phys. Rev. **D47** (1993), 3487.

[39] J.A. Gracey, Phys. Rev. **D86** (2012), 105029.

[40] S.P. Sorella, Annals Phys. **321** (2006), 1747.

[41] D. Zwanziger, Phys. Rev. **D81** (2010), 125027.

[42] A. Cucchieri, D. Dudal, T. Mendes & N. Vandersickel, arXiv:1405.1547.

[43] J.A. Gracey, Eur. Phys. J. **C70** (2010), 451.

[44] F.A. Behrends, A.I. Davydychev, V.A. Smirnov & J.B. Tausk, Nucl. Phys. **B439** (1995), 536.

[45] T. Kugo & I. Ojima, Prog. Theor. Phys. Suppl. **66** (1979), 1; Prog. Theor. Phys. Suppl. **71** (1984), 1121.

[46] T. Kugo, hep-th/9511033.

[47] V. Mader, M. Schaden, D. Zwanziger & R. Alkofer, Eur. Phys. J. **C74** (2014), 2881.

[48] A.C. Kalloniatis, L. von Smekal & A.G. Williams, Phys. Lett. **B609** (2005), 424.

[49] L. von Smekal, M. Ghiotti & A.G. Williams, Phys. Rev. **D78** (2008), 085016.

[50] P. Nogueira, J. Comput. Phys. **105** (1993), 279.

[51] J.A.M. Vermaseren, math-ph/0010025.

[52] M. Misiak & M. Münz, Phys. Lett. **B344** (1995), 308.

[53] K.G. Chetyrkin, M. Misiak & M. Münz, Nucl. Phys. **B518** (1998), 473.

[54] S. Laporta, Int. J. Mod. Phys. **A15** (2000), 5087.

[55] D.J. Broadhurst, J. Fleischer & O.V. Tarasov, Z. Phys. **C60** (1993), 287.

[56] C. Studerus, Comput. Phys. Commun. **181** (2010), 1293.

[57] C.W. Bauer, A. Frink & R. Kreckel, J. Symb. Comput, **33** (2002), 1.

[58] J. van der Bij & M. Veltman, Nucl. Phys. **B231** (1984), 205.

[59] C. Ford, I. Jack & D.R.T. Jones, Nucl. Phys. **B387** (1992), 373.

[60] A.I. Davydychev & J.B. Tausk, Nucl. Phys. **B397** (1993), 123.

[61] A.K. Rajantie, Nucl. Phys. **B480** (1996), 729; Nucl. Phys. **B513** (1998), 761.

[62] O.V. Tarasov & A.A. Vladimirov, Sov. J. Nucl. Phys. **25** (1977), 585.

[63] E. Egorian & O.V. Tarasov, Theor. Math. Phys. **41** (1979), 863.

[64] R.M. Doria, F.A.B. Rabelo de Carvalho & S.P. Sorella, Braz. J. Phys. **20** (1990), 316.

[65] J.A. Gracey, Phys. Lett. **B552** (2003), 101.

[66] R. Jackiw & S. Templeton, Phys. Rev. **D23** (1981), 2291.